

# POSTPRINT

## **A versatile room-temperature method for the preparation of customized fluorescent non-conjugated polymer dots**

**Lorenzo Vallan<sup>a</sup>, Esteban P. Urriolabeitia<sup>b</sup>, Ana M. Benito<sup>a</sup> and Wolfgang K. Maser<sup>a\*</sup>**

This is the un-edited version of the accepted manuscript published in

POLYMER

Reference: JPOL 21499

PII: S0032-3861 (19)30462-8

DOI: <https://doi.org/10.1016/j.polymer-2019.05.041>

Publication Date (on-line): 16 May 2019

# **A versatile room-temperature method for the preparation of customized fluorescent non-conjugated polymer dots**

**Lorenzo Vallan<sup>a</sup>, Esteban P. Urriolabeitia<sup>b</sup>, Ana M. Benito<sup>a</sup> and Wolfgang K. Maser<sup>a\*</sup>**

*<sup>a</sup>Instituto de Carboquímica (ICB-CSIC), C/Miguel Luesma Castán 4, E-50018 Zaragoza, Spain. \*Email: wmaser@icb.csic.es*

*<sup>b</sup>Instituto de Síntesis Química y Catálisis Homogénea (ISQCH-CSIC Universidad de Zaragoza), C/Pedro Cerbuna 12, E-50009 Zaragoza, Spain.*

## **ABSTRACT**

We present a general procedure for the synthesis and *in situ* functionalization of highly fluorescent non-conjugated polymer dots, by exploiting the room-temperature carbodiimide-mediated condensation between citric acid and amines. The versatility of this method is proved by the preparation and characterization of a broad set of fluorescent nanoparticles with customized polymer structures and functional groups.

**Keywords:** polymer dots • nanoparticles • fluorescence • synthesis • carbon dots

## **Introduction**

The fluorescence of polymer dots is widely ascribed to the presence of an extended  $\pi$ -conjugated polymer backbone comprised by repetitive units such as benzene, thiophene or carbazole. However, fluorescence has been reported also in several non-conjugated polymer dots (NCPDs), involving polymers such as poly(amidoamine) [1], polyurea [2], polycarbonate [3], polyacrylonitrile [4], polyurethane [5], poly(aminoester) [6-7] and modified polyethyleneimine [8-9]. Non-conjugated structures present several advantages over their conjugated relatives, including superior water solubility, biocompatibility and a rich surface

chemistry. Thanks to these properties, fluorescent NCPDs are excellent candidates for the preparation of sensors [5, 10], biosensors [11], imaging probes [9, 12-13] and drug nanocarriers [14-15].

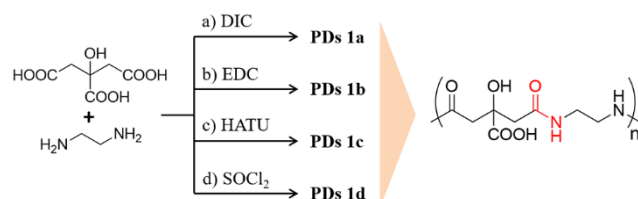
The fluorescence in NCPDs is the result of structural rigidity, whereby the loss of rotational and vibrational freedom of the polymer structure promotes the radiative relaxation pathway after the absorption of light. For a broad variety of NCPDs, the fluorescence is explained by the so-called aggregation-induced emission (AIE) effect [3-4, 6, 16-19]. Here the use of enhanced polymer concentrations leads to the formation of aggregated polymer clusters being able to satisfy the required condition of structural rigidity. Nevertheless, rigidity in NCPDs can be attained as an intrinsic feature of the particle's structure itself, for example by crosslinking polymers into a branched and rigid polymeric network. In this case, the fluorescence of NCPDs originates from the so-called crosslink enhanced emission (CEE) effect [20].

In the last years, the group of Bai Yang carried out extensive studies on the CEE effect in carbon dots [21-24], linking the bright blue fluorescence that is frequently observed for this class of nanoparticles to the high structural rigidity of their polymeric component [12]. Furthermore, our group recently demonstrated that the polycondensation between carboxylic acid and ethylenediamine is a sufficient condition for obtaining highly fluorescent nanoparticles, unravelling that intramolecular interactions and charge-transfer mechanism constitute the origin of the CEE effect [25]. Going a step further, in this work we develop a general and versatile method for the rational design and the *in situ* functionalization of highly fluorescent NCPDs. In here, the employment of a coupling agent controls the polycondensation between citric acid and a wide number of different amines in a room temperatures synthesis approach. The resulting NCPDs' structure is thus customized by the choice of reagents. Moreover, the *in situ* functionalization of the nanoparticles is easily

obtained by adding to the reaction any kind of nucleophilic amine, which acts as polymerization quencher and at the same time introduces the moiety desired for specific applications.

## Results and discussion

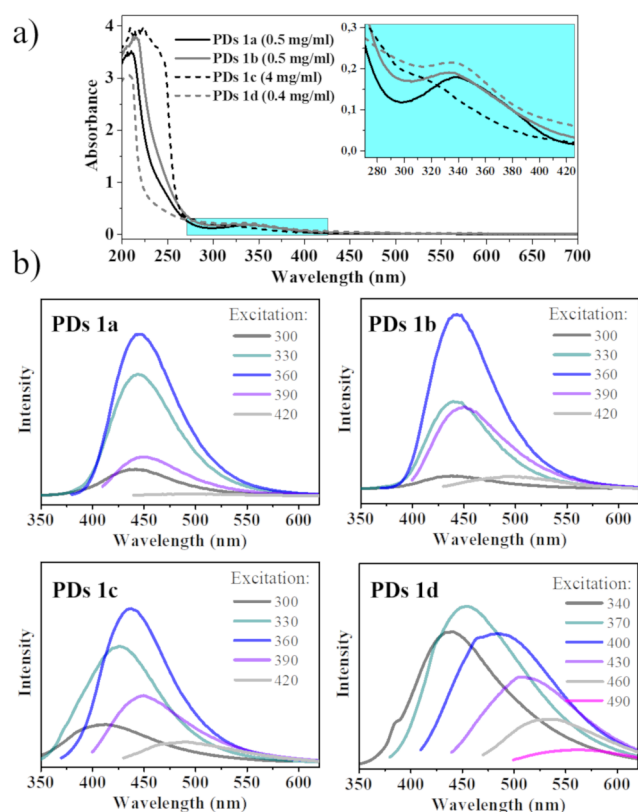
With the purpose to investigate the most effective approach for achieving the formation of fluorescent NCPDs by polycondensation, citric acid (CA) and ethylenediamine (EDA) in a ratio 1:1 were chosen for testing four different strategies (Scheme 1). This involves the carboxylic acid activation with a) *N,N'*-diisopropylcarbodiimide (DIC), b) *N*-(3-Dimethylamino-propyl)-*N'*-ethylcarbodiimide hydrochloride (EDC), c) hexafluorophosphate azabenzotriazole tetramethyl uronium (HATU) and the acyl chloride formation with d) thionyl chloride (for the procedures see the Supplementary Data).



**Scheme 1.** Polycondensation between CA and EDA through four synthetic pathways rendering **PDs 1a-d**. (single column figure)

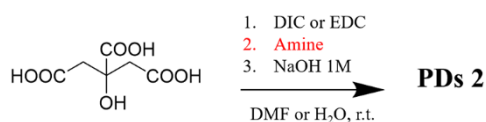
**PDs 1a-d** were characterized by atomic force microscopy (AFM, Fig. S3) and diffusion ordered spectroscopy (DOSY, Fig. S4 and Table S1). These techniques revealed that all the samples consist of nanoparticles of 1 and 2 nm in size. The structural characterization of **PDs 1a-1d** was performed by means of elemental analysis (Table S2 and Fig. S5), infrared (IR, Fig. S6-S9) and nuclear magnetic resonance (NMR) spectroscopy (Fig. S10-S25). Gathering all the structural information, it becomes evident that all the four methods employed accomplished the synthesis of NCPDs whose structure comprises the condensation products

of CA carboxylic acids and EDA amines. Despite of the structural similarity, an investigation of the **PDs 1a-1d** optical properties showed that the fluorescence intensity depends considerably on the synthetic method. UV/Vis spectra of **PDs 1a**, **PDs 1b** and **PDs 1d** present an absorption band at 340 nm, while for **PDs 1c** the same feature has its maximum at 310 nm (Fig. 1a). The emitting behavior of the four samples shows indeed a correlation with the quantum yield (QY). In **PDs 1a** (QY=17.7%) and **1b** (QY=8.6%) the emission takes place around 445 nm and is nearly independent of the excitation, while in **PDs 1c** and **1d** the QY is remarkably lower (respectively 2.2% and 4.0%) and exhibits an excitation-dependent emission (Fig. 1b). In order to explain these differences, it is important to emphasize that the fluorescent decay in this type of PDs originates from the high conformational rigidity achieved by intramolecular hydrogen bonding and electrostatic interactions [25]. Thus, in **PDs 1a and 1b** the establishment of the most stable and rigid conformation during the polymerization process provides the base for their higher QYs. Moreover, the conformational uniformity of the emitting states is reflected in their excitation-independent emission. On the contrary, the lower QYs and the excitation-dependent behavior of **PDs 1c** and **1d** suggest that the polymerization processes taking place are inefficient towards the achievement of the most rigid and stable folding conformation. Therefore, in these cases the excitation dependency can be ascribed to the conformational heterogeneity of the emitting centers.



**Fig. 1.** Absorption spectra of **PDs 1a-d**. b) Emission of **PDs 1a-d** for different excitation wavelengths. (single column figure)

Once confirmed that the DIC- and EDC- mediated condensation strategies are the most effective routes for the synthesis of highly fluorescent NCPDs from CA and EDA, in a next step, EDA was substituted by different types of aliphatic and aromatic polyamines. Maintaining the established reaction conditions, the synthesis of **PDs 2a-f** was accomplished (Scheme 2, Table 1).

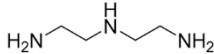
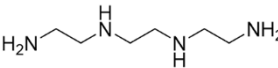
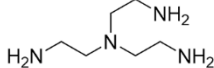
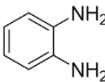
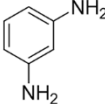
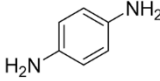



**Scheme 2.** Synthesis of **PDs 2a-f**. (single column figure)

The as-produced materials **PDs 2a-f** were characterized by AFM (Fig. S32) and DOSY (Fig. S33 and Table S3). Both techniques consistently reveal that all samples consist of nanoparticles with sizes between 1.0 and 2.5 nm, except for **PDs 2c**, which reveals a size of about 2 nm by AFM and of 4.8 nm by DOSY. The as produced materials were characterized by elemental analysis, IR, and NMR spectroscopy. Also for **PDs 2a-c**, the C, H, N and O percentages strongly suggest that the formed copolymers are made of CA and the employed amine in a 1:1 ratio (Tables S4-S6 and Fig. S34-S36). However, this stoichiometry is not preserved for **PDs 2d-f**, presumably due to the lower and co-dependent reactivity of the aromatic di-amines (Table S7 and Fig. S37), but also to the presence of unknown impurities (Fig. S56, S60, S64). IR spectra (Fig. S38-S43) show C=O stretching for carboxylic acids and amides, as previously observed for **PDs 1a-d**. Moreover, **PDs 2d-f** present the typical aromatic C-C stretching modes between 1516-1497 cm<sup>-1</sup> (Fig. S41-S43). Finally, <sup>1</sup>H, <sup>13</sup>C APT, <sup>1</sup>H-<sup>13</sup>C HSQC and <sup>1</sup>H-<sup>13</sup>C HMBC experiments confirmed the copolymer connectivity via amide as result of the condensation between citric acid and the respective amine (Fig. S44-67). For **PDs 2d-f** are also well visible the aromatic signals, between 7.5-6.5 ppm in the proton spectra and 147-109 ppm in the carbon spectra. The fact that the results of the structural characterization conclusively confirm the expected polyamide structures emphasizes the versatility of our synthetic procedure. Concerning the optical properties of **PDs 2a-f**, it is observed that their maximum emission intensity, which appears between 433 and 452 nm (Fig. S69-74), does not change consistently with the amine employed. On the other hand, the QY of **PDs 2a-c**, with aliphatic amines, is higher than in **PDs 2d-f**, with aromatic amines (Table 1). In fact, aliphatic amines exhibit a higher degree of conformational freedom with respect to aromatic amines, thus facilitating more easily the establishment of the intramolecular forces, which are responsible for the rigid and fluorescent conformation. However, the radiative decay is hampered by the locked configuration of the amines in o-, m-

or p- position on the aromatic ring. Among these, the o- position, due to its resemblance with the EDA conformation, should be the considered as the most favourable one. This assumption is further underlined by the observation that the QY of **PDs 2d** is higher than the one of **PDs 2e**, which in turn is higher than the one of **PDs 2f**, whose substituents' directionality does not enable the compact folding required for the formation of the fluorophore.

**Table 1.** Amines employed for the polycondensation, emission maximum, QY and pictures (in water, UV light off and on) of **PDs 2a-f**. (single column figure)

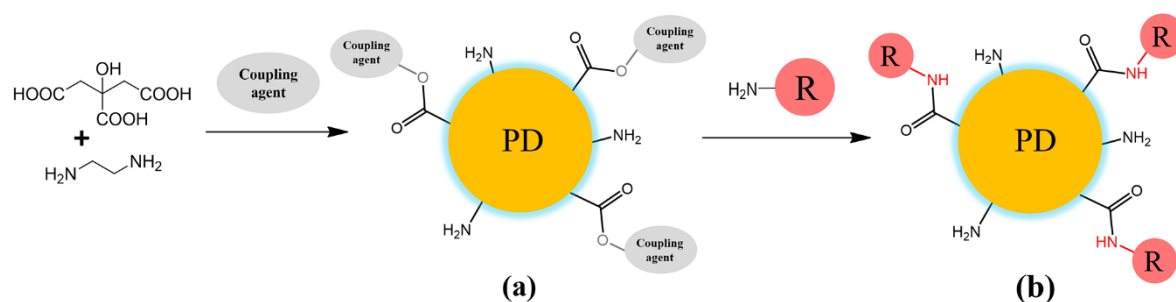
Sample	Amine	$\lambda_{em}$ (nm)	QY (%)
2a		443	24.5
2b		435	7.3
2c		452	4.7
2d		433	3.9
2e		440	1.6
2f		440	0.8

The finding that the polycondensation catalyzed by carbodiimides can be successfully exploited for the synthesis of different fluorescent nanoparticles as a function of the type of


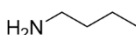
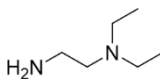
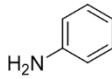
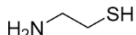
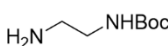


amine group employed, thus enables gaining control on their final chemical structure. It further provided a unique opportunity to perform an additional study for testing the possibility to functionalize by *in situ* approaches the as-produced materials. Since the growth of the nanoparticles is mediated by the activation of the carboxylic acids via coupling agents, it can be interrupted at any moment adding an excess of a strong nucleophile. In the previous experiments, NaOH was used to restore the carboxylic acids and quench the polymerization process. Nevertheless, primary amines are equally good candidates for this purpose. Moreover, the employment of an amine offers the possibility to attach onto the surface of the PDs virtually any moiety that is stable and soluble in the reaction medium. The *in situ* functionalization was tested by the addition of five different primary amines during the polycondensation reaction between CA and EDA mediated by DIC (Scheme 3, Table 2).




**Scheme 3.** a) Polycondensation of CA and EDA mediated by a coupling agent. b) Addition of a primary amine consuming the activated carboxylic acids and finishing the polymerization process. (two columns figure)

**Table 2.** Amine employed for the functionalization, emission maximum, QY and pictures (in water, UV light off and on) of **PDs 3a-e**. (single column figure)

Sample	H <sub>2</sub> N- 	$\lambda_{em}$ (nm)	QY (%)
3a		445	8.6
3b		445	8.4
3c		434	5.8
3d		433	25.2
3e		430	4.7



3a
3b
3c
3d
3e

Similarly to **PDs 1a-d**, **PDs 3a-e** reveal sizes between 1.0-2.6 nm, as probed by AFM (Fig. S76) and DOSY (Fig. S78, Table S8). Elemental analysis shows that the functionalized materials **PDs 3a-e** present lower molar percentages of oxygen compared to **PDs 1a**, being a consequence of the successful functionalization (Table S9 and Fig. S78). In parallel, in the infrared spectra of **PDs 3a-3d** (Fig. S79-S83) the carboxylic acid C=O stretching at 1704 cm<sup>-1</sup> is weaker than in **PDs 1a** or not visible at all, due to the consumption of the majority of the carboxyl groups upon their functionalization. In **PDs 3e** this effect is not appreciable because of the presence of the carbamate C=O stretching band, which is found at similar wavenumbers as the carboxylic one. Additionally, **PDs 3c** reveals the C-C stretching mode at

1545  $\text{cm}^{-1}$  related to its aromatic ring.  $^1\text{H}$ ,  $^{13}\text{C}$  APT,  $^1\text{H}$ - $^{13}\text{C}$  HSQC and  $^1\text{H}$ - $^{13}\text{C}$  HMBC experiments confirmed the introduction on **PDs 3a-3e** of the corresponding functionalities (Fig. S84-S103). Interestingly, different QY are obtained, depending on the type of functionalization. Here rigid and bulky groups, such as in **PDs 3c** and **3e**, decrease the fluorescence emission. In contrast, the QY benefits of the thiol functionalization, possibly due to its involvement in H-bond interactions that play a role in the formation of the polymer conformation required for attaining the fluorescent behavior. On the other hand, the structural modifications performed only slightly affect the absorption (Fig. S104) and emission maximum position (Fig. S105- S109), thus emphasizing a rather negligible role in the fluorescence mechanism. Finally, while the solubility of **PDs 1a-d** and **PDs 2a-f** is limited to aqueous media, **PDs 3a-e** were found to be soluble in ethanol, methanol, DMF and, specifically for **PDs 3a** and **PDs 3d**, also in dichloromethane. In fact, the functionalization on one side can introduce lipophilic moieties on the nanoparticles surface and, on the other, it causes the consumption of carboxylic acids, thus reducing the presence of ammonium carboxylate salts and improving the solubility in organic solvents.

## Conclusions

In summary, the presented method provides a highly versatile and simple strategy for the synthesis of novel highly fluorescent NCPDs with customized functionalities. The fluorescence is the result of the intrinsic structural rigidity of the as-produced nanoparticles. The synthesis procedure consists of the coupling agent-mediated polycondensation between citric acid and amines at room temperature and enables the formation of a wide variety of NCPDs whose polymer structure is defined by the choice of the reagents. Furthermore, the method facilitates the *in situ* functionalization of the NCPDs and enables an additional level of control towards their final chemical structure. Our method thus provides a valuable toolbox

for the design of a wide spectrum of polymer dots with controlled functionalities, thus enhancing their application potential in the field of sensors, fluorescent probes and drug nanocarriers.

## **Experimental Section**

Experimental details are reported in Appendix A. Supplementary data.

## **Conflict of interests**

There are no conflicts to declare.

## **Acknowledgements**

This project has received funding from the European Union's Horizon 2020 research and innovation programme under the Marie Skłodowska-Curie grant agreement No 642742. A.M.B., W.K.M acknowledge Spanish MINEICO (project grant ENE2016-79282-C5-1-R) and the Gobierno de Aragón (Grupo Reconocido DGA T03\_17R) and associated EU Regional Development Funds. E.P.U acknowledges the Gobierno de Aragón (Grupo Reconocido DGA E19-17R) and associated EU Regional Development Funds.

## **Appendix A. Supplementary data**

Supplementary data to this article can be found online at <https://doi.org/10.1016/j.polymer.2019.xx.xxx>.

## **References**

1. Lee, W. I.; Bae, Y.; Bard, A. J., Strong Blue Photoluminescence and ECL from OH-Terminated PAMAM Dendrimers in the Absence of Gold Nanoparticles. *J. Am. Chem. Soc.* **2004**, *126* (27), 8358-8359.

2. Restani, R. B.; Morgado, P. I.; Ribeiro, M. P.; Correia, I. J.; Aguiar-Ricardo, A.; Bonifácio, V. D. B., Biocompatible Polyurea Dendrimers with pH-Dependent Fluorescence. *Angew. Chem. Int. Ed.* **2012**, *51* (21), 5162-5165.
3. Huang, W.; Yan, H.; Niu, S.; Du, Y.; Yuan, L., Unprecedented strong blue photoluminescence from hyperbranched polycarbonate: From its fluorescence mechanism to applications. *J. Polym. Sci. A* **2017**, *55* (22), 3690-3696.
4. Zhou, Q.; Cao, B.; Zhu, C.; Xu, S.; Gong, Y.; Yuan, W. Z.; Zhang, Y., Clustering-Triggered Emission of Nonconjugated Polyacrylonitrile. *Small* **2016**, *12* (47), 6586-6592.
5. Tong, D.; Li, W.; Zhao, Y.; Zhang, L.; Zheng, J.; Cai, T.; Liu, S., Non-conjugated polyurethane polymer dots based on crosslink enhanced emission (CEE) and application in Fe<sup>3+</sup> sensing. *RSC Adv.* **2016**, *6* (99), 97137-97141.
6. Yuan, L.; Yan, H.; Bai, L.; Bai, T.; Zhao, Y.; Wang, L.; Feng, Y., Unprecedented Multicolor Photoluminescence from Hyperbranched Poly(amino ester)s. *Macromol. Rapid Commun.* **2019**, *0* (0), 1800658.
7. Shen, Y.; Ma, X.; Zhang, B.; Zhou, Z.; Sun, Q.; Jin, E.; Sui, M.; Tang, J.; Wang, J.; Fan, M., Degradable Dual pH- and Temperature-Responsive Photoluminescent Dendrimers. *Chem.–Eur. J* **2011**, *17* (19), 5319-5326.
8. Liu, S. G.; Liu, T.; Li, N.; Geng, S.; Lei, J. L.; Li, N. B.; Luo, H. Q., Polyethylenimine-Derived Fluorescent Nonconjugated Polymer Dots with Reversible Dual-Signal pH Response and Logic Gate Operation. *J. Phys. Chem. C* **2017**, *121* (12), 6874-6883.
9. Sun, Y.; Cao, W.; Li, S.; Jin, S.; Hu, K.; Hu, L.; Huang, Y.; Gao, X.; Wu, Y.; Liang, X.-J., Ultrabright and Multicolorful Fluorescence of Amphiphilic Polyethyleneimine Polymer Dots for Efficiently Combined Imaging and Therapy. *Sci. Rep.* **2013**, *3*, 3036.
10. Liu, S. G.; Luo, D.; Li, N.; Zhang, W.; Lei, J. L.; Li, N. B.; Luo, H. Q., Water-Soluble Nonconjugated Polymer Nanoparticles with Strong Fluorescence Emission for Selective and

Sensitive Detection of Nitro-Explosive Picric Acid in Aqueous Medium. *ACS Appl. Mater. Interfaces* **2016**, 8 (33), 21700-21709.

11. Zhao, J.; Dong, Z.; Cui, H.; Jin, H.; Wang, C., Nanoengineered Peptide-Grafted Hyperbranched Polymers for Killing of Bacteria Monitored in Real Time via Intrinsic Aggregation-Induced Emission. *ACS Appl. Mater. Interfaces* **2018**, 10 (49), 42058-42067.

12. Zhu, S.; Meng, Q.; Wang, L.; Zhang, J.; Song, Y.; Jin, H.; Zhang, K.; Sun, H.; Wang, H.; Yang, B., Highly Photoluminescent Carbon Dots for Multicolor Patterning, Sensors, and Bioimaging. *Angew. Chem. Int. Ed.* **2013**, 52 (14), 3953-3957.

13. Sun, B.; Zhao, B.; Wang, D.; Wang, Y.; Tang, Q.; Zhu, S.; Yang, B.; Sun, H., Fluorescent non-conjugated polymer dots for targeted cell imaging. *Nanoscale* **2016**, 8 (18), 9837-9841.

14. Xu, L.; Yeudall, W. A.; Yang, H., Folic acid-decorated polyamidoamine dendrimer exhibits high tumor uptake and sustained highly localized retention in solid tumors: Its utility for local siRNA delivery. *Acta Biomater.* **2017**, 57, 251-261.

15. Wang, H.-J.; He, X.; Luo, T.-Y.; Zhang, J.; Liu, Y.-H.; Yu, X.-Q., Amphiphilic carbon dots as versatile vectors for nucleic acid and drug delivery. *Nanoscale* **2017**, 9 (18), 5935-5947.

16. Zhao, E.; Lam, J. W. Y.; Meng, L.; Hong, Y.; Deng, H.; Bai, G.; Huang, X.; Hao, J.; Tang, B. Z., Poly[(maleic anhydride)-alt-(vinyl acetate)]: A Pure Oxygenic Nonconjugated Macromolecule with Strong Light Emission and Solvatochromic Effect. *Macromolecules* **2015**, 48 (1), 64-71.

17. Miao, X.; Liu, T.; Zhang, C.; Geng, X.; Meng, Y.; Li, X., Fluorescent aliphatic hyperbranched polyether: chromophore-free and without any N and P atoms. *Phys. Chem. Chem. Phys.* **2016**, 18 (6), 4295-4299.

18. Lu, H.; Feng, L.; Li, S.; Zhang, J.; Lu, H.; Feng, S., Unexpected Strong Blue Photoluminescence Produced from the Aggregation of Unconventional Chromophores in Novel Siloxane–Poly(amidoamine) Dendrimers. *Macromolecules* **2015**, *48* (3), 476-482.
19. Zhou, X.; Luo, W.; Nie, H.; Xu, L.; Hu, R.; Zhao, Z.; Qin, A.; Tang, B. Z., Oligo(maleic anhydride)s: a platform for unveiling the mechanism of clusteroluminescence of non-aromatic polymers. *J. Mater. Chem. C* **2017**, *5* (19), 4775-4779.
20. Zhu, S.; Wang, L.; Zhou, N.; Zhao, X.; Song, Y.; Maharjan, S.; Zhang, J.; Lu, L.; Wang, H.; Yang, B., The crosslink enhanced emission (CEE) in non-conjugated polymer dots: from the photoluminescence mechanism to the cellular uptake mechanism and internalization. *Chem. Commun.* **2014**, *50* (89), 13845-13848.
21. Zhu, S.; Song, Y.; Shao, J.; Zhao, X.; Yang, B., Non-Conjugated Polymer Dots with Crosslink-Enhanced Emission in the Absence of Fluorophore Units. *Angew. Chem. Int. Ed.* **2015**, *54* (49), 14626-14637.
22. Tao, S.; Song, Y.; Zhu, S.; Shao, J.; Yang, B., A new type of polymer carbon dots with high quantum yield: From synthesis to investigation on fluorescence mechanism. *Polymer* **2017**, *116*, 472-478.
23. Tao, S.; Zhu, S.; Feng, T.; Xia, C.; Song, Y.; Yang, B., The polymeric characteristics and photoluminescence mechanism in polymer carbon dots: A review. *Mater. Today Chem.* **2017**, *6*, 13-25.
24. Tao, S.; Lu, S.; Geng, Y.; Zhu, S.; Redfern, S. A. T.; Song, Y.; Feng, T.; Xu, W.; Yang, B., Design of Metal-Free Polymer Carbon Dots: A New Class of Room-Temperature Phosphorescent Materials. *Angew. Chem. Int. Ed.* **2018**, *57* (9), 2393-2398.
25. Vallan, L.; Urriolabeitia, E. P.; Ruipérez, F.; Matxain, J. M.; Canton-Vitoria, R.; Tagmatarchis, N.; Benito, A. M.; Maser, W. K., Supramolecular-Enhanced Charge Transfer

within Entangled Polyamide Chains as the Origin of the Universal Blue Fluorescence of Polymer Carbon Dots. *J. Am. Chem. Soc.* **2018**, *140* (40), 12862-12869.

## TOC

